

Communication

An Electro-Optic, Actively Q-Switched Tm:YAP/KGW External-Cavity Raman Laser at 2273 nm and 2344 nm

Rotem Nahear, Neria Suliman, Yechiel Bach and Salman Noach *

Department of Applied Physics, Electro-Optics Engineering Faculty, Jerusalem College of Technology, Jerusalem 9372115, Israel; rotem.nahear@mail.huji.ac.il (R.N.); nsuliman@g.jct.ac.il (N.S.); ybach@g.jct.ac.il (Y.B.)

* Correspondence: salman@jct.ac.il

Abstract: This paper presents a KGW Raman laser with an external-cavity configuration in the 2 μm region. The Raman laser is pumped by unique, electro-optic, actively Q-switched Tm:Yap laser, emitting at 1935 nm. The electro-optic modulation is based on a KLTN crystal, enabling the use of a short crystal length, with a relatively low driving voltage. Due to the KGW bi-axial properties, the Raman laser is able to lase separately at two different output wavelengths, 2273 and 2344 nm. The output energies and pulse durations for these two lines are 0.42 mJ/pulse at 18.2 ns, and 0.416 mJ/pulse at 14.7 ns, respectively. This is the first implementation of a KGW crystal pumped by an electro-optic active Q-switched Tm:Yap laser in the SWIR spectral range.

Keywords: solid state laser; 2 μm laser; Raman laser; KGW crystal; active Q-switch; electro-optics



Citation: Nahear, R.; Suliman, N.; Bach, Y.; Noach, S. An Electro-Optic, Actively Q-Switched Tm:YAP/KGW External-Cavity Raman Laser at 2273 nm and 2344 nm. *Photonics* **2021**, *8*, 519. <https://doi.org/10.3390/photronics8110519>

Received: 20 October 2021

Accepted: 17 November 2021

Published: 19 November 2021

Publisher's Note: MDPI stays neutral with regard to jurisdictional claims in published maps and institutional affiliations.



Copyright: © 2021 by the authors. Licensee MDPI, Basel, Switzerland. This article is an open access article distributed under the terms and conditions of the Creative Commons Attribution (CC BY) license (<https://creativecommons.org/licenses/by/4.0/>).

1. Introduction

Lasers emitting at 2–3 μm enhance a wide variety of applications because of their relatively high absorption coefficients and the interesting atmospheric window at this spectral range. They are used in LIDAR; microsurgery [1]; the processing of polymers, semiconductors, and metals [2]; defense applications; and gas sensing industries [3]. However, SWIR solid-state laser technology, especially in the region of 2–3 μm , has yet to be fully mature, currently relying on a limited range of doped-crystalline and rare-earth ions, such as thulium, holmium, and chromium. The current technology allows the generation of laser sources in part of the 2–3 μm spectral range, but does not cover it entirely.

Raman lasers leverage the principles of stimulated Raman scattering (SRS) to shift the light that comes into the crystal by a frequency corresponding to the vibrational frequency of the material. Pumping Raman cavities at very high peak power densities enables frequency conversion and produces new laser lines and useful high-brightness sources. This extends the spectral spans of existing lasers and fills the spectral gaps in this spectral range [4–7]. Raman lasers have a few more advantages, such as linewidth narrowing, pulse length shortening, and spatial beam quality improvement through Raman beam cleanup [8].

The gain of a Raman laser is dependent on the pump intensity and the gain coefficient of the Raman crystal material. There are only a few publications on Raman lasers in the 2 μm region, mainly for two reasons. The first is the lack of suitable high power pump sources for this spectral range. The second is the decrease in the Raman gain coefficient at longer wavelengths, which is approximately proportional to inverse wavelength. The result of these two reasons is lower efficiency Raman lasers compared to VIS and NIR.

The first demonstrations of SRS conversion in 2 μm using Tm:KY(WO₄)₂ and BaWO₄ crystals were reported more than a decade ago [9,10]. However, these reports are missing the information about the obtained output energy values. Since 2013, several studies have demonstrated crystalline Raman lasers in the 2–4 μm region: A BaWO₄ crystal pumped by a Tm:YAP laser emitting at 2360 nm achieved 0.31 mJ of output energy [11], a YVO₄ crystal pumped by a Tm:YAP laser emitting at 2418 nm yielded 0.27 mJ of output energy [12],

a BaWO₄ crystal pumped by a Tm, Ho:GdVO₄ laser emitting at 2533 nm obtained 0.31 mJ of output energy [13,14], and a BaWO₄ crystal pumped by a Ho:YAG laser emitting at 2602 nm yielded 0.27 mJ of output energy [15]. A more recent publication has introduced a Raman laser based on a diamond crystal, which has the highest Raman gain coefficient, pumped by a Tm:YLF at 1.89 μm emitting at 2.52 μm. They achieved up to 1.67 mJ of output energy per pulse [7], but with a very low repetition rate.

From this overview, it can be seen that the BaWO₄ crystal is the favorite Raman crystal to generate a wavelength shift at this spectral range due to their relatively high Raman gain value. Diamond can also be considered as a good crystal due to its high Raman gain, but it suffers from multiphoton absorption, which limits the wavelength range. The highest conversion efficiency of these works was 13.9% (6.8% efficiency from pump diode, for intracavity lasers), except for the diamond, which achieved a high conversion efficiency of 38%, but with limited average power at around 8 mW at a slow repetition rate of 5 Hz.

Another well-known Raman crystal is potassium gadolinium tungstate (KGd(WO₄)₂ or KGW), owing to its good optical and thermal properties. KGW has a high damage threshold, and its negative thermo-optic coefficient mitigates the onset of thermal lensing compared to other Raman crystals [4,16]. Moreover, because KGW is biaxial, it has Raman interactions with two different vibrational modes (768 and 901 cm⁻¹), yielding the option to obtain two different Stokes wavelengths by controlling the polarization of the pump [16]. Generally, KGW has been mainly used in the visible and 1 μm spectral range because of its initial lower Raman gain value (3–4 at 1064 nm compared to 16 at the BaWO₄) and the dependence of the Raman gain coefficient lowering with increasing wavelength.

Since the SRS is a non-linear process and therefore requires high power density, the pump source should be pulsed. Usually it is implemented by actively Q-switching, which can be manifested either by acousto-optic (AO) or electro-optic (EO) modulators. The acousto-optic modulator (AOM) is characterized by high-power consumption and a relatively long switching time due to the traveling duration of the acoustic wave in the crystal. Compared to the AOM, the electro-optic modulator (EOM) has a faster switching time, allowing shorter pulses. However, the voltage required for its operation is high and directly proportional to the laser wavelength, which increases the operation complexity of the EOM at long wavelengths [17].

The EO crystals used in EOM which are suitable for 2 μm lasers are RTP and LiNbO₃. In practice, there are only a few reports on diode-pumped, all-solid-state EO, Q-switched 2 μm lasers that work at room temperature. In one such report from 2016, a diode pumped laser system with a Tm:YAG slab laser crystal, using an RTP-based EOM, achieved 7.5 mJ with 58 ns pulse duration [18]. In 2018, a diode-pumped Tm:LuAG laser using a LiNbO₃ crystal based EOM delivered a pulse energy of 10.8 mJ with a pulse width of 52 ns [19]. In both cases, the EO crystals were exceptionally long and were operated with an extremely high voltage, significantly complicating the cavity design and supporting electronics. For example, using a LiNbO₃ at the 2 μm wavelength range requires a 25 mm long crystal, and an operating voltage of 3 kV, as reported in [19].

In 2018 we reported the first Raman laser in the 2 μm region based on a KGW crystal. The KGW Raman laser was pumped by an actively Q-switched Tm:YLF laser based on an AOM which operated at 1880 nm [20]. The reasons for choosing the KGW crystal, despite its low Raman gain coefficient compared to the BaWO₄, were its good thermal properties and its relatively higher damage threshold. By using our Tm-based seed we can achieve a good Raman conversion.

The active Q-switch mechanism of the pump source is unique in two main aspects. The EO crystal is KLTN, and the switching mechanism is polarization modulation. The KLTN is an unique perovskite crystal, with a quadratic EO effect in the paraelectric phase [21]. Near the crystal ferroelectric phase transition, the electro-optic effect is significantly increased, which allows large reductions in the driving voltage and the crystal length.

The switching is done by a novel method developed to mitigate the strong piezoelectric ringing in the KLTN, and to allow more stable pulses at higher repetition rates.

The novelty of this work is in the implementation of the above new EO modulator as an active Q-switch in the Tm:YAP pump laser (emit at 1935 nm), together with a KGW crystal in order to extend the variety of output wavelengths while utilizing Raman effect in this spectral range. When using the Tm:YAP laser as a pump source, we need to cooperate with its relatively high thermal lensing constraints, in order to improve the Raman laser's performance.

The KGW Raman laser operated at two different wavelengths. At the first operating wavelength of 2273 nm, we obtained the output energy of 0.42 mJ/pulse and 18.2 ns pulse duration. At the second wavelength of 2344 nm, energy of 0.416 mJ/pulse was reached; however, a shorter pulse duration of 14.7 ns was measured. To the best of our knowledge, this is the first Raman laser in the 2 μ m region demonstrating the combination of an EO modulation Tm:YAP pump laser and a KGW Raman crystal.

2. Experimental Setup

The Raman laser was built up in an external cavity configuration, which unlike the intracavity configuration, does not limit the design of the pump laser, and allows one to achieve both high energy and short pulse duration. This configuration is more reliable regarding design considerations and alignment constraints. It facilitates the control of the pump power density in the Raman crystal by proper design of the delivering optics between the fundamental and Raman lasers. In addition, with this architecture, it is easier to achieve mode matching and proper thermal management, since the two cavities are separated.

The experimental setup of the Raman laser and its fundamental pump source is shown in Figure 1. The pump laser was an EO actively Q-switched Tm:YAP laser. The EOM operated with the polarization modulation method that was described in detail in a previous study [22]. The cavity included a 10 mm length a-cut Tm:YAP (3% at.) crystal with a $3 \times 3 \text{ mm}^2$ cross-section, as a gain medium, end-pumped by a 30 W, 793 nm laser-diode. The pump beam was focused to a beam diameter of 330 μ m inside the Tm:YAP crystal. Both the diode and Tm:YAP crystal were water-cooled to 18 $^{\circ}$ C. A plano-concave mirror with a 200 mm radius of curvature (ROC) was used as an input mirror, having an AR coating at the pump wavelength, and a high reflectance (HR) coating at 1850–2000 nm. A plano-concave mirror with a 100 mm ROC was used as an output coupler (OC) with a partially reflecting (PR) coating of 55% reflectance for the 1850–2000 nm. The cavity length was 150 mm. The EOM was based on a KLTN electro-optic crystal. The crystal had a trapezoidal shape to reduce acoustic waves inside the crystal. The KLTN crystal was 2 mm long, and the clear aperture was $3 \times 3 \text{ mm}^2$. The KLTN crystal was installed in a temperature-controlled holder that maintained its temperature at 6 degrees above the phase transition temperature. A quarter wave plate (QWP) was inserted between the Tm:YAP and the KLTN. When the QWP axes was tilted 45 $^{\circ}$ with respect to the crystals axes the modulator was in "off" state. an uncoated yttrium aluminum garnet (YAG) etalon plate, with 100 μ m thickness, was inserted into the laser cavity to narrow the laser spectral line. The lasing wavelength was measured to be 1935 nm. The pulse duration was measured to have a 19 ns full width at half-maximum (FWHM). The laser beam was linearly p-polarized.

The output beam from the Tm:YAP was imaged by a pair of antireflective (AR) coated, plano-convex lenses, to a spot diameter of \sim 220 μ m in the center of the KGW crystal. Due to the divergence of the beam, the beam size increased to \sim 300 μ m at the facets of the Raman crystal.

A half-wave-plate (HWP) was added between the lenses to control the polarization orientation and enable switching between the two different Raman vibration shifts of the KGW crystal, thereby enabling selective lasing at 2273 and 2344 nm. Such an external cavity configuration is advantageous for a two-wavelength Raman laser, since it allows for easy switching between the two Raman-shifted modes.

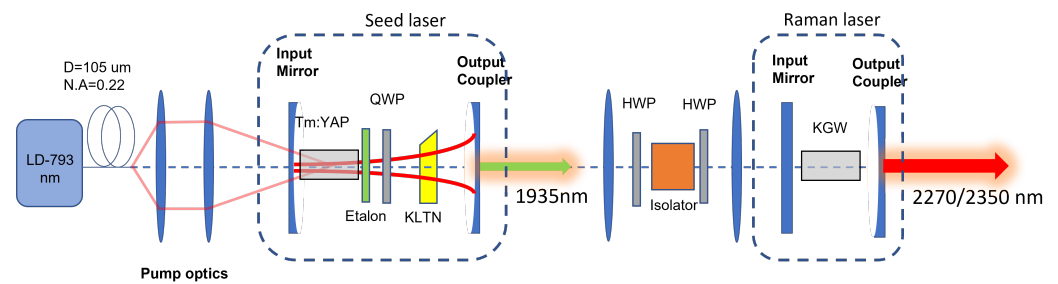


Figure 1. Experimental setup of the external KGW Raman laser and its actively Q-switched Tm:YAP seed laser.

A plano-plano mirror, AR coated for 1860–1960 nm and HR coated for 2170–2700 nm, was used as an input mirror for the Raman laser cavity, and a plano-concave mirror with a 100 mm ROC was used as an OC. This mirror had a PR-coating of 93% reflectance between 2170 and 2450 nm and HR coating for 1850–1960 nm, enabling double-pass pumping of the 30 mm long KGW crystal, which was used as the active Raman medium. The crystal was AR coated for the fundamental and Raman wavelengths, and its cross-section was $7 \times 7 \text{ mm}^2$. This crystal was oriented for propagation along the b-axis, having 901 cm^{-1} shift and 768 cm^{-1} shift, for E (electric field) perpendicular to the c-axis and a-axis, respectively, [16]. As mentioned before, the control of the electric field polarization was facilitated using the HWP. The total Raman laser cavity length was 34 mm. The Raman beam waist diameter inside the KGW crystal was calculated by the ABCD matrix method to be $350 \mu\text{m}$. This mode matching (between the seed and the Raman laser) was found to be highly efficient.

The pulse energy was measured by an energy meter (Ophir, PE50-C). Pulse temporal characterization was performed using an extended InGaAs fast photodetector with 200 ps rise-time (Alphasas, UPD-5N-IR2-P) and an oscilloscope (Tektronix, AFG3102C). The laser spectrum was acquired by a spectrometer (APE, Wavescan).

3. Results and Discussion

The Raman laser output spectrum for each of the first two Stokes shifts is shown in Figure 2. Raman lasing at 2273 nm was observed for the 768 cm^{-1} shift, and emission at 2344 nm was observed for the 901 cm^{-1} shift. The two lines were observed for orthogonal orientations of the fundamental laser polarization with respect to each other at the KGW crystal, as expected from the theory.

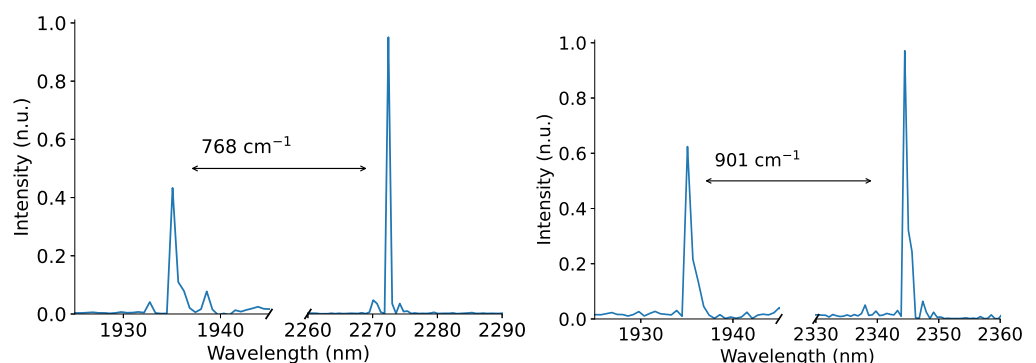


Figure 2. The two Raman spectral shifts of 768 cm^{-1} (left) and 901 cm^{-1} (right). The fundamental laser and Raman laser were measured separately.

Figure 3 presents the output energies and pulse durations of the two different Raman shifts, as functions of the pulse energy of the fundamental pump laser at a 0.5 kHz repetition rate. For both Raman lines, a threshold of 1.26 mJ/pulse from the fundamental laser was measured. At the highest available pump energy of 1.7 mJ/pulse, a maximum output

energy of 0.42 mJ/pulse was attained at 2273 nm, corresponding to a conversion efficiency of 24.8% and average power of 210 mW; and 0.416 mJ/pulse was attained at 2344 nm, corresponding to a conversion efficiency of 24.4% and average power of 208 mW. The pulse duration at 2273 nm was 18.2 ns FWHM, corresponding to a peak power of 23 kW; and at 2344 nm the pulse duration was 14.7 ns FWHM, corresponding to a peak power of 28.3 kW. The temporal profiles of the pulses are presented in Figure 4.

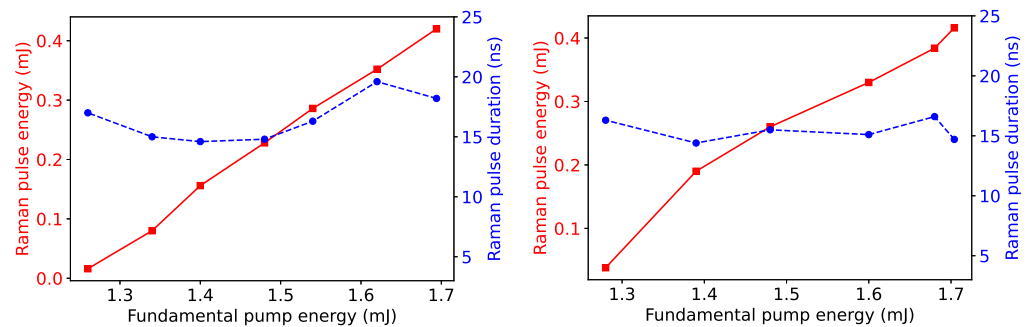


Figure 3. Energy per pulse (square) and pulse duration (circle) of the two Raman shifts: at 2273 nm on the (left) and at 2344 nm on the (right).

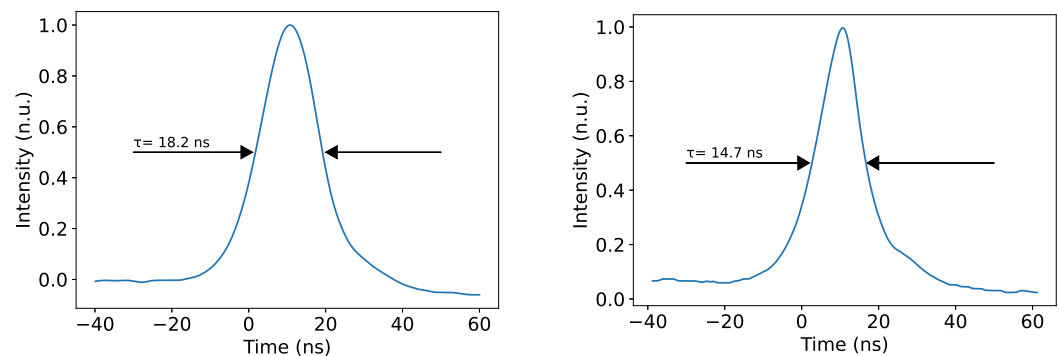


Figure 4. Temporal profiles of the two Raman shifts: at 2273 nm (left) and 2344 nm (right).

From Figure 3, the rising of the Raman energy as function of the seed pulse energy can be seen. In both polarizations, this rising is continuous throughout the graph. This is in contrast to a previous work in our laboratory where the rising stopped when the Raman energy reached 0.32 mJ [23]. In both works, the seed was emitted at the same wavelength (1935 nm) and used the same Raman crystal; however, the seed in this work was actively Q-switched, and the seed in the other work was passively Q-switched. A possible explanation for the difference could be the difference in the repetition rate: in this work the repetition rate was 0.5 kHz, whereas the repetition rate in the former work was 1 kHz, which generated double the number of phonons. Perhaps the saturation behavior in one of the polarizations in the former work can be explained by the higher amount of heat generated in the crystal compared to the experiment reported herein.

Regarding to the variation in the Raman pulse duration as a function of the seed pulse energy, there are conflicting considerations: On one hand, the higher the seed pulse intensity, the higher the Raman gain, which leads to rapid building of the pulse and a short pulse duration. On the other hand, the higher the seed pulse intensity, the longer the effective seed pulse duration (the part of the pulse with power above the Raman threshold, which is high since it is a nonlinear process), leading to a longer Raman pulse duration. This trade-off may explain the inconsistent behavior of the Raman pulse duration as a function of the seed pulse energy, as presented in Figure 3.

The beam quality of the seed was measured at low power in the CW configuration, and the calculated M^2 was 1.1. The Raman beam quality was not measured, since the

high peak power made it difficult to measure it. However, according to the theory [24], the Raman process usually arises from the main modes of the beam, and therefore, the beam quality is better than in the pump. From this theory, it can be assumed that if the seed's beam quality is initially good, the Raman beam quality will not be worse. The Raman laser's best results are summarized in Table 1.

Table 1. KGW Raman laser's maximal performances for the two Raman Stokes shifts.

Shift	Wavelength	Energy	Pulse Duration	Peak-Power	Efficiency	Power
768 cm ⁻¹	2273 nm	0.42 mJ/pulse	18.2 ns	23 kW	24.8%	210 mW
901 cm ⁻¹	2344 nm	0.416 mJ/pulse	14.7 ns	28.3 kW	24.4%	208 mW

4. Conclusions

In conclusion, an efficient laser for SRS wavelength conversion in the 2 μm region using an external cavity configuration was presented. To the best of our knowledge, this was the first implementation of all-solid-state Raman laser based on a KGW crystal as a gain medium with a KLTN based, electro-optic, active Q-switched Tm:YAP laser. A KGW pumped by an 1935 nm displayed spectral shifting of two distinct output wavelengths at 2273 and 2344 nm. The laser exhibited the highest energy of 0.42 mJ/pulse yet reported for the 2 μm spectral regime using Raman conversion at the first Stokes wavelength. In addition to its optical, mechanical, and thermal properties, and based on the comprehensive use of this crystal at shorter wavelengths, the use of the KGW was also expanded to longer wavelengths in the 2 μm spectral regime. This active Q-switch Raman laser could be suitable for many new 2 μm applications, though it demands, during firing, controlled repetition rates and high peak power.

Author Contributions: Investigation, R.N., N.S. and Y.B.; Supervision, S.N. All authors have read and agreed to the published version of the manuscript.

Funding: This research received no external funding.

Acknowledgments: The authors thank Professor Agranat from the Hebrew University of Jerusalem for the electro-optic modulator. The authors would like to thank David Sinefeld from JCT, for their fruitful insights to the scope of this publication.

Conflicts of Interest: The authors declare no conflict of interest.

References

- Serebryakov, V.; Boško, É.; Kalintsev, A.; Kornev, A.; Narivonchik, A.; Pavlova, A. Mid-IR laser for high-precision surgery. *J. Opt. Technol.* **2015**, *82*, 781–788. [[CrossRef](#)]
- Mingareev, I.; Weirauch, F.; Olowinsky, A.; Shah, L.; Kadwani, P.; Richardson, M. Welding of polymers using a 2 μm thulium fiber laser. *Opt. Laser Technol.* **2012**, *44*, 2095–2099. [[CrossRef](#)]
- Godard, A. Infrared (2–12 μm) solid-state laser sources: A review. *Comptes Rendus Phys.* **2007**, *8*, 1100–1128. [[CrossRef](#)]
- Piper, J.A.; Pask, H.M. Crystalline raman lasers. *IEEE J. Sel. Top. Quantum Electron.* **2007**, *13*, 692–704. [[CrossRef](#)]
- Černý, P.; Jelínková, H.; Zverev, P.G.; Basiev, T.T. Solid state lasers with Raman frequency conversion. *Prog. Quantum Electron.* **2004**, *28*, 113–143. [[CrossRef](#)]
- Pask, H.M. The design and operation of solid-state Raman lasers. *Prog. Quantum Electron.* **2003**, *27*, 3–56. [[CrossRef](#)]
- Demetriou, G.; Kemp, A.J.; Savitski, V. 100 kW peak power external cavity diamond Raman laser at 2.52 μm. *Opt. Express* **2019**, *27*, 10296–10303. [[CrossRef](#)]
- Sabella, A.; Piper, J.A.; Mildren, R.P. Efficient conversion of a 1.064 μm Nd: YAG laser to the eye-safe region using a diamond Raman laser. *Opt. Express* **2011**, *19*, 23554–23560. [[CrossRef](#)]
- Basiev, T.; Basieva, M.; Doroshenko, M.; Fedorov, V.; Osiko, V.; Mirov, S. Stimulated Raman Scattering in the Mid IR Range 2.31–2.75–3.7 μm in a BaWO₄ Crystal under 1.9 and 1.56 μm Pumping. In Proceedings of the Advanced Solid-State Photonics, Incline Village, NV, USA, 29 January–1 February 2006; p. MB10.
- Batay, L.; Kuzmin, A.; Grabtchikov, A.; Lisinetskii, V.; Orlovich, V.; Demidovich, A.; Titov, A.; Badikov, V.; Sheina, S.; Panyutin, V.; et al. Efficient diode-pumped passively Q-switched laser operation around 1.9 μm and self-frequency Raman conversion of Tm-doped KY(WO₄)₂. *Appl. Phys. Lett.* **2002**, *81*, 2926–2928. [[CrossRef](#)]

11. Zhao, J.; Li, Y.; Zhang, S.; Li, L.; Zhang, X. Diode-pumped actively Q-switched Tm: YAP/BaWO₄ intracavity Raman laser. *Opt. Express* **2015**, *23*, 10075–10080. [[CrossRef](#)]
12. Cheng, P.; Zhao, J.; Xu, F.; Zhou, X.; Wang, G. Diode-pumped mid-infrared YVO₄ Raman laser at 2418 nm. *Appl. Phys. B* **2018**, *124*, 1–5. [[CrossRef](#)]
13. Zhao, J.; Zhang, X.; Guo, X.; Bao, X.; Li, L.; Cui, J. Diode-pumped actively Q-switched Tm, Ho: GdVO₄/BaWO₄ intracavity Raman laser at 2533 nm. *Opt. Lett.* **2013**, *38*, 1206–1208. [[CrossRef](#)] [[PubMed](#)]
14. Zhang, X.; Ding, Y.; Qiao, Y.; Li, G.; Cui, J. Diode-end-pumped efficient 2533 nm intracavity Raman laser with high peak power. *Opt. Commun.* **2015**, *355*, 433–437. [[CrossRef](#)]
15. Kuzucu, O. Watt-level, mid-infrared output from a BaWO₄ external-cavity Raman laser at 2.6 μm. *Opt. Lett.* **2015**, *40*, 5078–5081. [[CrossRef](#)] [[PubMed](#)]
16. Mochalov, I.V. Laser and nonlinear properties of the potassium gadolinium tungstate laser crystal KGd(WO₄)₂: Nd³⁺-(KGW: Nd). *Opt. Eng.* **1997**, *36*, 1660–1669. [[CrossRef](#)]
17. Wang, X.; Basseras, P.; Miller, R.D.; Sweetser, J.; Walmsley, I. Regenerative pulse amplification in the 10-kHz range. *Opt. Lett.* **1990**, *15*, 839–841. [[CrossRef](#)]
18. Jin, L.; Liu, P.; Huang, H.; Liu, X.; Shen, D. Short pulse diode-pumped Tm: YAG slab laser electro-optically Q-switched by RbTiOPO₄ crystal. *Opt. Mater.* **2016**, *60*, 350–354. [[CrossRef](#)]
19. Guo, L.; Zhao, S.; Li, T.; Yang, K.; Qiao, W.; Li, D.; Li, G.; Zhang, S.; Bian, J.; Zheng, L.; et al. Diode-wing-pumped electro-optically Q-switched 2 μm laser with pulse energy scaling over ten millijoules. *Opt. Express* **2018**, *26*, 17731–17738. [[CrossRef](#)] [[PubMed](#)]
20. Sheintop, U.; Sebbag, D.; Komm, P.; Pearl, S.; Marcus, G.; Noach, S. Two-wavelength Tm: YLF/KGW external-cavity Raman laser at 2197 nm and 2263 nm. *Opt. Express* **2019**, *27*, 17112–17121. [[CrossRef](#)] [[PubMed](#)]
21. Gumennik, A.; Kurzweil-Segev, Y.; Agranat, A.J. Electrooptical effects in glass forming liquids of dipolar nano-clusters embedded in a paraelectric environment. *Opt. Mater. Express* **2011**, *1*, 332–343. [[CrossRef](#)]
22. Noach, S.; Nahear, R.; Vidal, Y.; Garcia, Y.; Agranat, A.J. Electro-optic active Q-switched Tm: YLF laser based on polarization modulation. *Opt. Lett.* **2021**, *46*, 1971–1974. [[CrossRef](#)] [[PubMed](#)]
23. Perez, E.; Sheintop, U.; Nahear, R.; Marcus, G.; Noach, S. Efficient all-solid-state passively Q-switched SWIR Tm: YAP/KGW Raman laser. *Opt. Lett.* **2020**, *45*, 5409–5412. [[CrossRef](#)] [[PubMed](#)]
24. Murray, J.T.; Austin, W.L.; Powell, R.C. Intracavity Raman conversion and Raman beam cleanup. *Opt. Mater.* **1999**, *11*, 353–371. [[CrossRef](#)]